Biosensors and Bioelectronics 262 (2024) 116560

Contents lists available at ScienceDirect

Biosensors and Bioelectronics

journal homepage: www.elsevier.com/locate/bios

Assessing the performance of a robust multiparametric wearable patch integrating silicon-based sensors for real-time continuous monitoring of sweat biomarkers

Meritxell Rovira [a], Céline Lafaye [b], Silvia Demuru [c], Brince Paul Kunnel [c], Joan Aymerich [a], Javier Cuenca [a], Francesc Serra-Graells [a,f], Josep Maria Margarit-Taulé [a], Rubaiyet Haque [c,1], Mathieu Saubade [b,d], César Fernández-Sánchez [a,e], Cecilia Jimenez-Jorquera [a,*]

[a] Instituto de Microelectrónica de Barcelona (IMB-CNM), CSIC, Bellaterra, Spain
[b] Swiss Olympic Medical Center, Lausanne University Hospital, Lausanne, Switzerland
[c] École Polytechnique Fédérale de Lausanne (EPFL), Switzerland
[d] Center for Primary Care and Public Health (Unisanté), University of Lausanne, Lausanne, Switzerland
[e] Centro de Investigación Biomédica en Red de Bioingeniería, Biomateriales y Nanomedicina (CIBER-BBN), Madrid, Spain
[f] Dept. of Microelectronics and Electronic Systems, Universitat Autònoma de Barcelona, Spain

ARTICLE INFO

Keywords:
Wearable sensor
Sweat biomarker
Microfabricated sensor
Capillary-based fluidics
Healthcare
Fitness management

ABSTRACT

The development of wearable devices for sweat analysis has experienced significant growth in the last two decades, being the main focus the monitoring of athletes health during workouts. One of the main challenges of these approaches has been to attain the continuous monitoring of sweat for time periods over 1 h. This is the main challenge addressed in this work by designing an analytical platform that combines the high performance of potentiometric sensors and a fluidic structure made of a plastic fabric into a multiplexed wearable device. The platform comprises Ion-Sensitive Field-Effect Transistors (ISFETs) manufactured on silicon, a tailor-made solid-state reference electrode, and a temperature sensor integrated into a patch-like polymeric substrate, together with the component that easily collects and drives samples under continuous capillary flow to the sensor areas. ISFET sensors for measuring pH, sodium, and potassium ions were fully characterized in artificial sweat solutions, providing reproducible and stable responses. Then, the real-time and continuous monitoring of the biomarkers in sweat with the wearable platform was assessed by comparing the ISFETs responses recorded during an 85-min continuous exercise session with the concentration values measured using commercial Ion-Selective Electrodes (ISEs) in samples collected at certain times during the session. The developed sensing platform enables the continuous monitoring of biomarkers and facilitates the study of the effects of various real working conditions, such as cycling power and skin temperature, on the target biomarker concentration levels.

1. Introduction

During the practice of exercise, body thermoregulatory action results in the production of sweat, which is composed of 99 % water, electrolytes like sodium (Na^+), potassium (K^+) and chloride (Cl^-) ions together with metabolites like urea, pyruvate and lactate. The reliable measurement of such biomarkers would be a valuable asset in personalized health assessment for the prevention of adverse health effects due to dehydration (Neal et al., 2016; D. S. D.S. Yang et al., 2023). Among the biomarkers present in sweat, Na^+, K^+ and Cl^- are physiologically relevant, as their loss has a great impact on body fluid balance (Bariya et al., 2018). Their concentrations shift between 1 mM — 100 mM for Na^+ and Cl^-, and 1 mM — 18.5 mM for K^+. Monitoring pH levels, which usually range between 3 and 8, can also reflect changes in the concentration of various electrolytes in sweat, and thus help in the assessment of the athlete's metabolic state (Sonner et al., 2015; Yokus et al., 2020).

This need for personalized and *in situ* health assessment is pushing the use of portable and rapid analytical devices, like the commercial ISEs

* Corresponding author.
E-mail address: cecilia.jimenez@csic.es (C. Jimenez-Jorquera).
[1] Current affiliation: Dept. of Mathematics and Physics, North South University, Dhaka-1229, Bangladesh.

https://doi.org/10.1016/j.bios.2024.116560
Received 20 May 2024; Received in revised form 28 June 2024; Accepted 7 July 2024
Available online 11 July 2024

from Horiba, Ltd, which provide reliable discrete measurements. Some studies report the good accuracy of these devices for sweat analysis (Baker, 2017; Baker et al., 2014, 2022; Rollo et al., 2021; Wang et al., 2022; Zhang et al., 2019). However, while they show excellent performance, their geometry and size make them unsuitable for integration in on-body real-time monitoring systems.

Although sweat is an easily accessible biofluid, its production is very slow and very small sample volumes can be collected for analysis in a short period of time. Indeed, exercise-induced sweat is typically segregated in the range of 0.5–1.4 μL cm^{-2} min^{-1} (Buono et al., 2010). Thus, real-time and continuous analysis of sweat requires the use of analytical platforms able to perform using low sample volumes. Several compact and wearable platforms have been reported in the last decade to address this challenge (Ghaffari et al., 2021; Min et al., 2023). Those based on electrochemical sensors were first published in 2010 by Diamond's group. They developed a Na^+ ISE wearable device, applied to measuring concentration changes of this target species during exercise carried out by patients suffering from cystic fibrosis and healthy individuals (Schazmann et al., 2010). Since then, different research groups have been working on the development of wearable devices for the aforementioned sweat biomarker detection (Anastasova et al., 2017; Cazalé et al., 2016; Parrilla et al., 2016; Pirovano et al., 2020; M. Yang et al., 2023; Zhao et al., 2019).

Most wearable electrochemical sensor devices reported so far are based on the application of inkjet printing or screen-printing technologies to produce ISEs directly on flexible substrates (Ghaffari et al., 2021; Golparvar et al., 2023; Matzeu et al., 2015; Nakata et al., 2017; Xu et al., 2019). These show the advantages of fabrication simplicity and cost-effectiveness, as well as easy adaptability to the body. However, they often suffer from a lack of reproducibility and electronic noise due to substrate bending and stretching under moving conditions. Besides, most of them do not incorporate fluidic approaches to continuously drive the sweat to the sensing areas, being thus applied for single measurements.

Silicon-based sensors produced by microfabrication technologies are promising alternatives for this purpose, showing small size and enabling the integration with various interfacing electronic readouts being compatible with complementary metal-oxide-semiconductor (CMOS) technology (Cao et al., 2023). They are usually highly robust devices, and as such can be used for continuous monitoring during long-term exercise practices. The integration of silicon sensors in wearable devices was first described by Temple-Boyer's group, who integrated an ISE and an ISFET for Na^+ detection in a flexible substrate also containing the reference electrode (RE) (Cazalé et al., 2016). This device was tested on-body at different heat exposures, showing a correlation between sweat Na^+ concentration and body temperature. The integration of ISFETs onto flexible polyethylene terephthalate (PET) substrates together with a temperature probe has been described by Takei's group (Nakata et al., 2017), demonstrating the potential of this technology and the feasible compensation of the effect of temperature on the ISFET pH measurements in sweat. Ionescu's group (Garcia-Cordero et al., 2018) highlighted the importance of implementing small sensing areas for sweat analysis and reported a 3D-ultralow volume SU-8 microfluidic approach that integrated a pH, Na^+ and K^+ CMOS ISFET array. The good performance of this platform was assessed for Na^+ and K^+ detection in standard aqueous solutions. More recently, the same group reported a 3D extended metal gate ISFET array fabricated with CMOS technology to be potentially used in sweat analysis and showing the low power requirements of this type of sensors (Zhang et al., 2019).

The described reports evidence that the main challenge still lies in the fabrication of a wearable platform that integrates different ISFET sensors with the required sensitivity and robustness to be applied on-body. Likewise, sensors should show a superior performance in terms of response stability, reproducibility and reusability that the ISFET sensors show when packaged onto conventional printed circuit boards (PCBs). Although advances have been made in this direction, the existing ISFET-based sensing systems have not yet demonstrated to enable continuous and real-time monitoring of different biomarkers in low-flow-rate sweat samples for more than 1 h. In this work, we demonstrate the feasibility of using silicon-based pH, Na^+, and K^+ ISFET sensors combined with an integrated reference electrode, a temperature sensor, and a fluidic structure for the continuous monitoring of sweat secreted by a subject carrying out static cycling exercise. The performance of the sensors incorporated into the wearable patch is compared with results gathered with commercial ISEs in collected samples, in order to demonstrate the feasibility of the developed wearable platform for the continuous monitoring of biomarkers for full exercise sessions.

2. Experimental section

2.1. Reagents and solutions

All reagents and solutions used in the preparation and characterization of the pH, Na^+, and K^+ ISFET sensors are described in the Supporting Information (SI).

2.2. Devices and equipment

Si-based chips (3 × 3 mm^2 size), including a Si_3N_4 gate-based ISFET and a metal-oxide-semiconductor field-effect transistor (MOSFET), were fabricated on silicon on insulator (SOI) 4-inch wafers (Fig. 1A), at the clean room facilities of the Institute of Microelectronics of Barcelona according to standard microfabrication techniques, following the protocol previously reported by the group (Jimenez-Jorquera et al., 2010). ISFET chips were diced, wire-bonded and either packaged on a rigid PCB strip for analytical characterization (Muñoz et al., 1996), or on the flexible substrate to produce the patch-like device, as described below. Custom-made polymeric membranes were deposited on the gate of the ISFET devices to produce the sensors for Na^+ and K^+, following the procedure described in the SI. A 3 × 3.5 mm^2 Pt microelectrode, also fabricated using standard photolithographic/etching processes (Gutiérrez-Capitán et al., 2015), was used for producing the solid-state RE. The preparation of the RE is described in the SI and a scheme and images of its layers are shown in Fig. 1B. A temperature sensor was also included in the wearable platform and consisted of a commercial 10 kOhm thermistor (Saitama Murata Manufacturing, Kyoto, Japan).

Measurements with sensors integrated into the patch were performed with custom-made read-out electronics (6 cm × 4 cm). The system containing the read-out and the patch is illustrated in Fig. 1C. Further information on the equipment for potentiometric measurements is described in the SI.

For the analysis of the sweat samples, commercial ISEs for Na^+, K^+ and pH (LAQUAtwin Na-11, K-11 and pH-11, from HORIBA Advanced Techno Co., Ltd., Kyoto, Japan) were used.

2.3. Fabrication of the wearable patch

The wearable patch integrating the sensor chips (pH, Na^+ and K^+ ISFETs, a temperature sensor and a reference microelectrode) is shown in Fig. 1C. Our approach comprises a 2.5 cm × 4.6 cm flexible PCB fabricated on a 0.1 mm-thick polyimide (PI) substrate. Contact areas for fixing and wire bonding the different chips, the electrical tracks and contact pads were defined. 18 μm-thick electrical copper tracks were coated with a thin gold layer on the contacts and pads. The wires were protected with a water-resistant, flexible polymer (Epoxy resin Deloduopox® CR8021), which exhibited excellent adhesion to the substrate. Whatman® filter paper grade 4 (Sigma-Aldrich), whose extremely fast filtering capacity is reported by the provider, and 0.5 mm-thick polyethylene/polypropylene (PE/PP) and 0.6 mm thick PE hydrophilic fibre layers kindly supplied by Porex Technologies GmbH (Aachen, Germany) were used for the fluidic components and patterned with a CO_2-laser cut system (Epilog Mini 24, Epilog Laser, United States). Three structures

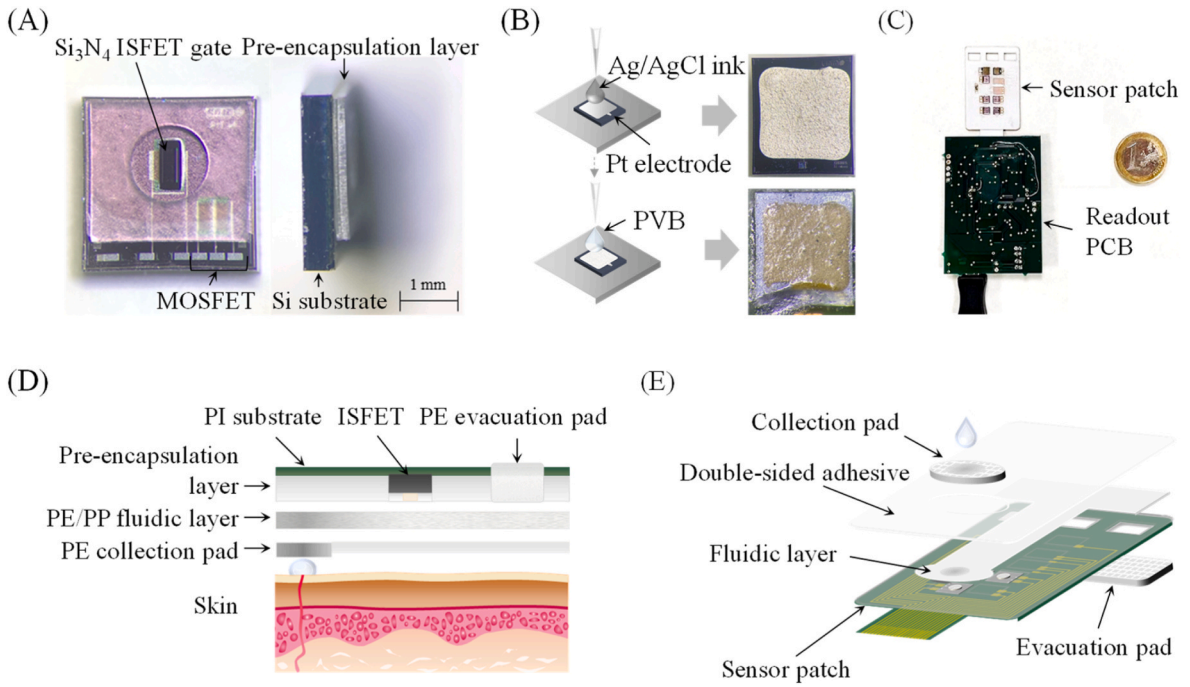

Fig. 1. Pictures and drawings of the components integrated in the wearable patch. (A) Top (left) and side (right) images of an ISFET. (B) Scheme of the Ag/AgCl and polyvinyl butyral (PVB) layers deposited on-chip to produce the solid-state reference electrode, and image of the actual chip. (C) Picture of the wearable device, including the sensor patch, and the readout electronics. (D) Exploded scheme of the wearable device in contact with the skin. (E) Drawing of the different layers of the wearable platform.

were patterned: a first oval-shaped pad for sweat collection in contact with the skin (d_1 5.5 mm, d_2 11.0 mm), a 6.4 mm width T-shaped microfluidic channel in contact with the sensors and an evacuation pad (22.7 mm × 7.9 mm) open to the environment, which facilitates continuous transport and constant sweat renewal on the areas over the sensors where measurements were recorded (Fig. 1D). Finally, an ARcare 90,445 double-sided medical-grade adhesive (Adhesives Research Inc., United States) was used to tightly fix the microfluidic components to the PCB substrate and ensure efficient adhesion of the wearable patch to the skin. The patch structure is depicted in Fig. 1E.

2.4. Sensor characterization methodologies

To determine pH, Na^+ and K^+ ISFETs parameters, calibrations were performed in deionized water and artificial sweat solutions spiked at different analyte concentrations. The methodologies are described in the SI. Open circuit potential (OCP) measurements were carried out in different solutions containing NaCl to evaluate the solid-state RE, using it as a working electrode in front of a double-junction commercial RE.

2.5. On-body evaluation

Exercise sessions were organized depending on the purpose, and their protocols are definded in the SI. The sessions were always performed in a laboratory at the Swiss Olympic Medical Center of the Lausanne University Hospital (CHUV) (Lausanne, Switzerland) following protocols approved by the ethical commission of the Canton of Vaud in accordance with the ethical standards laid down in the 1964 Declaration of Helsinki.

3. Results and discussion

3.1. Study of sensor performance in aqueous solutions

Sensors mounted on PCB strips were first used for calibration purposes in deionized water or buffered background solutions and in a set of *ad hoc* solutions containing the target analytes in a wide concentration range. As shown in Table S3 in SI, the sensors showed a nearly Nernstian response in a large concentration range covering the physiological ion content in sweat. The limits of detection (LODs) were below the lowest concentrations of these ions found in sweat (10^{-8} M for H^+ and 10^{-3} M for Na^+ and K^+), indicating that any change in their physiological range could be detected with the sensor devices. All these values were in agreement with previous data reported with these sensors when working under similar experimental solutions (Gutierrez et al., 2010; Jimenez-Jorquera et al., 2010).

The reversibility of the sensor responses was evaluated by studying the hysteresis of the voltage signal obtained when sequentially changing the target ion concentrations from low to high concentrations, and *vice versa*. The corresponding recordings are plotted in Fig. 2A. The maximum potential variation for the same concentration was 5.6 mV for pH, 3.2 mV for Na^+ and 3.0 mV for K^+. These variations can be related to the sensor memory effects and temporal drifts. The average variation was between 5 and 10% of the sensor sensitivity and could be considered negligible. For all the sensors, the response time, representing the duration required to attain 95% of the stable potential, was less than 5 s.

To identify sweat compounds that could affect the accuracy of the detection, potential interferents were added to different solutions containing a fixed concentration of the target ion. The sensors were immersed in the solutions containing relevant sweat compounds, and also in solutions with a different concentration of the target ion to check the sensor sensitivity. The recordings of the tests are plotted in Fig. 2B. For pH ISFET, the solution containing glucose did not produce a significant signal variation, as expected. However, the addition of the Na^+ and Ca^{2+}, produced a slight change in the potential due to the already known interfering effect (Esashi and Matsuo, 1978). The addition of the main groups of substances did not contribute to changes in the potential signal of Na^+ ISFETs. For K^+ ISFET, the interference of these compounds was low, being the vitamins the group that had the highest effect, and producing a 5.7 mV potential variation. The potential of Na^+ and K^+

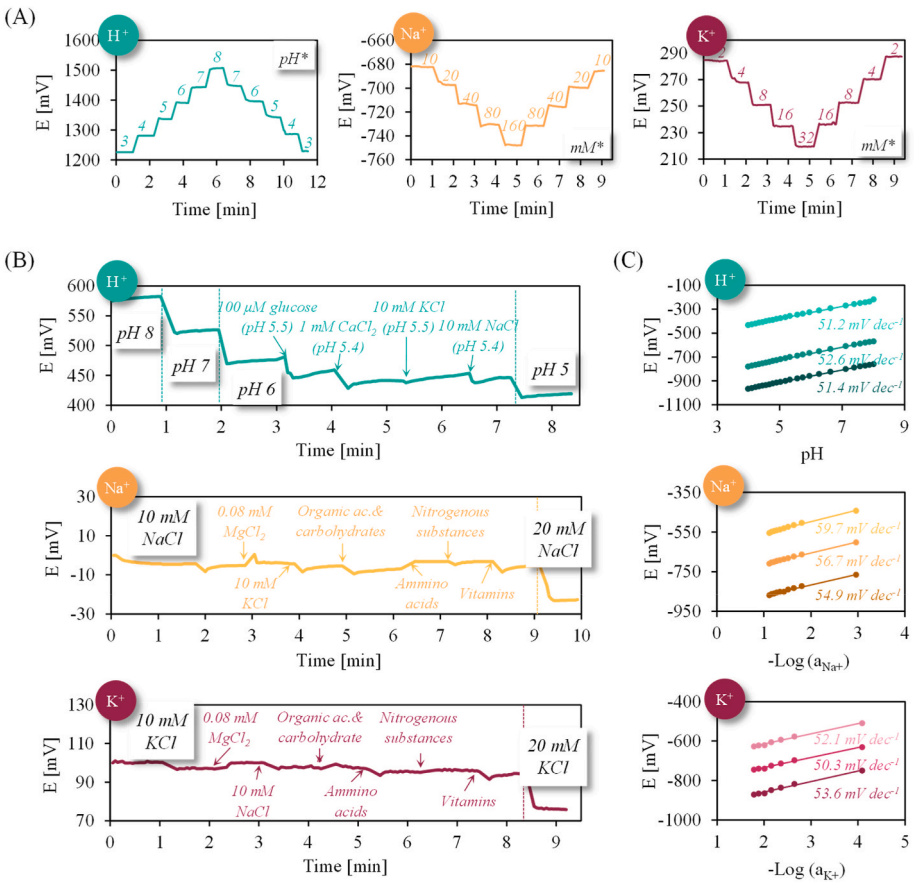

Fig. 2. Sensor performance in different aqueous solutions. (A) Recording of hysteresis responses of the pH, Na^+, and K^+ ISFET sensors in aqueous solutions. (B) pH, Na^+, and K^+ ISFET sensor responses when potential interfering substances that may be present in human sweat were added to the measuring solution. Data recording was temporarily paused in between every solution exchange. (C) Calibration curves of three pH, Na^+, and K^+ sensors in artificial sweat solutions.

ISFETs in the prepared solutions differed by a maximum of 2.5 mV and 5.7 mV, respectively, from the solution containing only the target analyte. Considering that their sensitivity to Na^+, and K^+ resulted in 60.0 mV dec^{-1}, and 65.1 mV dec^{-1}, the variation would correspond to less than 10% of the measured concentration. The pH ISFET maximum potential difference was 9.0 mV. According to the results, the changes in the potential output caused by the interfering substances were much smaller than those produced by the target analytes, which indicated the high specificity of the sensors.

An artificial sweat solution (whose composition is detailed in Tables S1 and SI) was used to fully assess the sensor analytical performance. Calibration curves were performed with three sensors for each target analyte in a range that covered the average concentrations found in sweat (Fig. 2C). For pH, Na^+, and K^+ ISFETs mean sensitivities of 51.7 ± 0.8, 57.1 ± 2.4, and 52.0 ± 1.6 mV dec^{-1} (N = 3) were obtained in artificial sweat solutions. The low standard deviations of the estimated sensitivity values indicate adequate reproducibility for pH, Na^+, and K^+ ISFETs. Additional characterization findings by the authors, as reported in (Rovira et al., 2023), further confirm the potential of the Na^+ ISFET in sweat sensing applications and indicate a sensor lifespan of more than one month.

The tailor-made solid-state Ag/AgCl/PVB RE was fully characterized. The results, presented in the SI, demonstrated adequate working stability for long-term sessions with the optimized REs comprising three layers of PVB. The stability of this RE in artificial sweat solutions containing different concentrations of K^+, Na^+, Cl^- and NO_3^- showed a signal variation of ±0.97 mV, thus confirming the high stability of the RE.

3.2. Characterization of the sensing platform with the fluidic components

Two material types were compared for the disposable capillary-based fluidic layer: a Whatman® fast filter paper and a PE/PP fiber film. Electrolyte solutions were driven through both materials, previously cut in a design that covered the sensors, and the PE/PP fiber layer showed 18-times higher linear speed, being the most adequate for on-body real-time measurements. Images of the test are shown in Fig. S4 in the SI.

The sensors were packaged in a patch-like platform and their performance with the fluidic components and the integrated solid-state RE (Fig. 3A) was compared with that of the same patch without fluidic elements and using an external RE. The calibration curves for pH, Na^+, and K^+ ISFETs in both situations are depicted in Fig. 3B. It should be noted that the calibration curves are overlapped, showing sensitivity differences of 0.03, 1.00, and 1.66 mV dec^{-1} for pH, Na^+, and K^+ ISFETs, respectively. This indicated efficient ion transfer from the fluidic structure to the ISFETs gate.

The sample renewal and the reversibility of the signal were assessed. The device was evaluated at a high flow rate of 100 µL min^{-1} using a syringe pump to replicate the continuous secretion of sweat, and positioned vertically, as would be on an athlete's back. The setup is illustrated in Fig. 3C. Three calibration solutions were successively pumped through the system, and the most diluted solution was injected at the end of the calibration. From the test results, presented in Fig. 3D, we could conclude that the solutions were driven continuously in real-time, the dilution front was small, the signal was stable regardless of the vertical orientation, no leakage occurred, the signals were reversible, and that the sensor patch could be reusable.

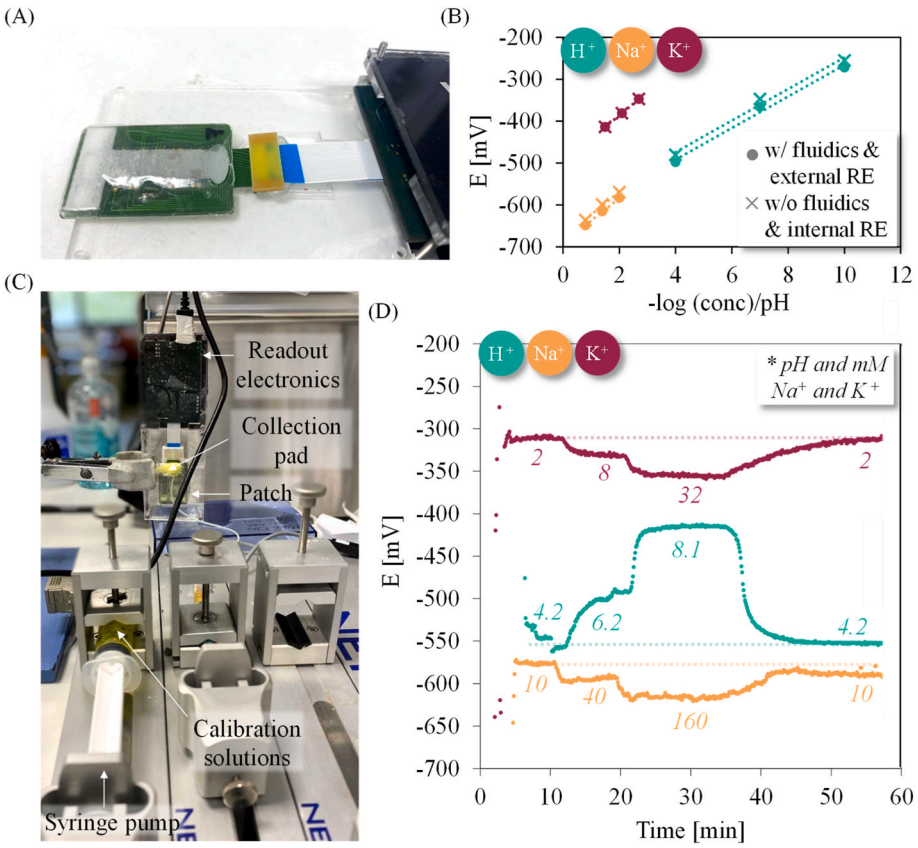

Fig. 3. Sensing platform setup images and responses to different tests. (A) Picture of the sensor patch tested using the PE/PP fluidic component. (B) Calibration curves obtained for pH, Na^+, and K^+ ISFETs integrated in the patch under two different experimental conditions. 1. An external RE was used and the sensors were covered with a drop of solution (without (w/o) fluidics); 2. An integrated RE was used and solutions were drived to the sensor areas using the fluidic component (with (w/) fluidics). (C) Image of the set-up used to assess the sensor reversibility test using the PE/PP fluidic component. (D) Responses of the pH, Na^+, and K^+ ISFET sensor integrated in the device together with the fluidic component, when artificial sweat solutions with different ion contents were sequentially pumped.

3.3. Determination of the best on-body location of the patch device

Sweat samples were collected during ten exercise sessions to assess the influence of the collection body part in Na^+ and K^+ concentration values. Statistical analyses were performed using Student's t-test, Tukey's honest significance test, and analysis of variance (ANOVA) test, where the significance level was set at $\alpha = 0.05$. Data was segregated based on the body area where samples were collected. A notable 20% variation between body areas was observed in the concentrations of each target analyte. This variation was closely examined to determine the optimum location for the sweat patch.

Comparative analysis using the paired *t*-test on Na^+ and K^+ concentrations collected at symmetrical positions on the body revealed no significant differences (t_{calc} 0.99 < t_{crit} 2.13 for both Na^+ and K^+). Consequently, these data from could be combined. The evaluated dataset is presented in Tables S4 and S5 in the SI. In order to examine the concentration differences in the samples collected at the different body locations, Tukey's honest significance test was applied to the dataset. Results confirmed that nearly all the samples compared with the ones collected on the torso or the arms showed significant differences in both Na^+ and K^+ mean concentration values. To visually depict the variations among body areas, the mean concentrations from different parts were represented in Fig. 4A and B. The connecting segments in the figures indicated significantly different groups, with their lengths reflecting the

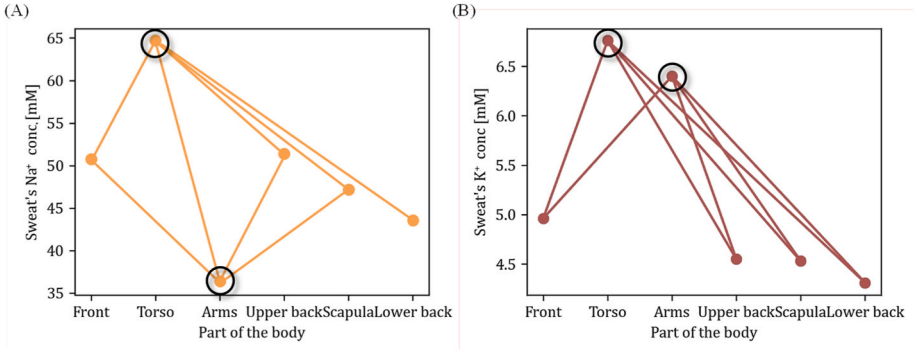

Fig. 4. Average sweat Na^+ (A), and K^+ (B), concentration values recorded during different sessions and effort stages, grouped into the body parts at which they were extracted, with significant differences represented using segments (95% confidence).

magnitude of differences observed.

Among the samples collected from other locations, including front, upper back, scapula and lower back, a closer examination revealed that the variability among the samples, quantified as the standard deviation, was notably lower for the lower back samples. Furthermore, high sweat rates were observed in this location (0.85 ± 0.41 mg cm^{-2}) (Patterson et al., 2000). Therefore, the lower back was selected as the preferred location for conducting on-body prototype tests.

3.4. On-body evaluation of the wearable patch

The patch device was finally tested on-body for 85 min of a cycling session (Fig. 5A). A leap forward was done in the current work with respect to the previously reported in (Wang et al., 2023), where Na^+ and K^+ concentrations in sweat were recorded during a session, by also measuring pH, skin temperature, the cycling power and the heart rate, in order to obtain more accurate physiological information. Before placing the patch on the subject's back, the integrated sensors were calibrated with three calibration solutions in artificial sweat. The sensors were calibrated again after the session. ISFETs potentials were recorded with a 10-s sampling rate during this session and discrete concentration values were calculated with the calibration plots recorded after the session. Moreover, sweat samples were collected every 10 min and analyzed with commercial ISEs.

First, two datasets were extracted from the recordings: the discrete concentrations at the time when the samples were collected, and the average of the recorded concentrations during the 5-min period before collecting the samples. Both datasets were compared with the samples concentrations provided by the commercial ISEs. The percentage errors resulting from the use of both discrete and mean ISFET concentrations are depicted in Fig. 5B. The mean percentage error across the samples, referred to as bias, together with the confidence intervals (CIs), are represented as lines in the plot for each biomarker.

Upon examining the pH results, low relative errors, most of them below 10%, were estimated. Average percentage errors as small as 3.5% and 2.6% were calculated from discrete and averaged ISFET values, respectively. As both of them included the 0 value within the 95% CIs (−2.4 – 9.3% for discrete and −2.0 – 7.2% for average values), we could conclude that the values recorded with the ISFET sensors were not biased. Regarding the comparison between both methods, although the average errors showed a close similarity, differences in precision were visible. The errors derived from discrete values exhibited some dispersion, while the majority of errors from averaged data fell within the established CI.

For Na^+ concentrations, the mean relative errors were −17.3% for discrete values and −20.3% for averaged values, and the 95% CIs fell below 0 (−31.7 to −2.9% for discrete and −27.4 – 13.1% for average values), indicating the presence of systematic errors. In this scenario, and unlike measurements performed for the other biomarkers, the averaged data exhibited a higher relative error. The subsequent analysis confirmed this behaviour.

Finally, K^+ ISFET's concentrations exhibited mean biases of −24.7% using discrete values and −21.1% using averaged data. Once more, the 95% CIs did not encompass 0 (−37.8 to −11.6% for discrete and −39.6 – 2.6% for average values), indicating a bias in the K^+ determination.

A systematic error observed in Na^+ and K^+ determinations was likely attributable to the matrix interference with the ion-selective polymeric membranes. This could be solved by an in-depth study focused on optimizing the membrane composition or by applying machine learning tools and neuronal networks, which might correct the signal after training (Margarit-Taulé et al., 2022).

The information obtained through the real-time data was analyzed in

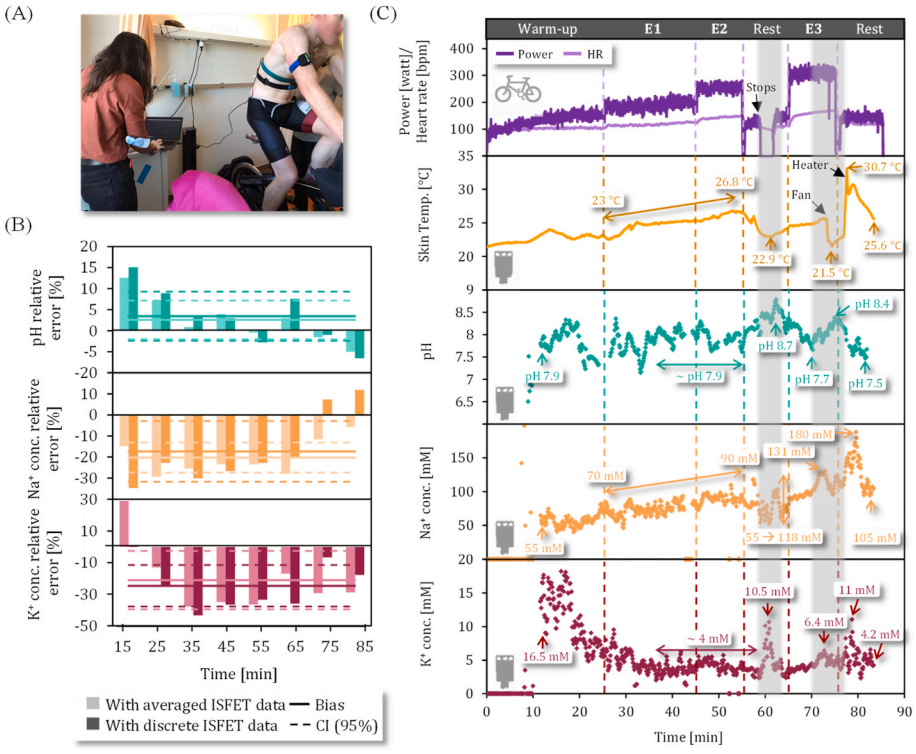

Fig. 5. On-body test of the wearable device. (A) Photograph of the volunteer wearing the device during the performance assessment session. (B) Relative errors of the pH, Na^+ and K^+ concentrations estimated from the recorded potentials of the ISFET sensors at the time when the sample collection pad was removed from the back of the volunteer and mean values recorded with the ISFETs over the 5-min time span in between sample collection events. (C) Recorded values of the different parameters tested during the ergocycle exercise of the volunteer at different exercise intensities (warm-up, E1, E2, E3 and rest). Recordings include cycling power, heart rate, skin temperature and pH, Na^+ and K^+ ISFETs concentration readings. Sweat biomarkers concentrations at particular times, are labelled. Grey areas define time periods influenced by different external inputs.

detail. Fig. 5C shows the concentration recorded with the sensors, together with the recordings of the skin temperature, the cycling power and the heart rate along the different exercise intensity stages of the session. The moments where some external factors may have influenced the measurements, such as the subject getting off the bicycle or being exposed to a fan or a heater, have been tagged.

First, for the warm-up session, it was observed that the initial time for the sensors to respond was about 15 min, meaning the time that it took the collected sweat to reach the sensors. After that, the signal of the pH and Na^+ sensors stabilized, and sweat was started to be sampled every 10 min to be analyzed off-body with the commercial ISEs. Initially, concentrations of 55 mM Na^+, 16.5 mM K^+, and a pH of 7.9 were calculated. A higher K^+ concentration than the expected one was observed, potentially indicating skin contamination, a common occurrence reflected by unusually high K^+ concentrations (>8 mM) previously reported (Weschler, 2008). At that juncture, the sample volume was minimal, making any electrolyte leached from the skin *stratum corneum* disproportionately impactful on the sample ion concentration. The K^+ concentration reverted to typical concentration levels (2–8 mM) (Baker and Wolfe, 2020) during the warm-up stage.

During E1 and E2 stages, skin temperature rose from 23 to 26.8 °C due to the power increase, while pH remained relatively constant. Once a substantial sweat rate was achieved (midway through E1), the K^+ concentration stabilized (~ 4 mM) until external conditions changed, as expected (Schwartz and Thaysen, 1956). At that point, the pH also stabilized at a 7.9 value, indicating proper sample flow within the microfluidic component to reach the pH ISFET gate. Moreover, during E1 and E2 stages, Na^+ concentration steadily increased, from 70 to 90 mM Na^+, in the same direction as the effort and sweat rate. These results are in accordance with the extensively reported dependence of Na^+ concentration on sweat rate (Sato, 1977; Sonner et al., 2015).

Between E2 and E3 stages, the subject stopped the exercise and got off the bicycle. This interruption was denoted by a decline in skin temperature (down to 22.9 °C), an unsteady Na^+ signal fluctuating from 55 to 118 mM and a sudden increase in K^+ concentration that reached 10.5 mM. These fluctuations were believed to result from stopping the sweat flow, leading to a phenomenon akin to that observed at the initial stage of the monitoring. Upon the beginning of the E3 stage, the Na^+ and K^+ ISFETs potential values returned to those recorded at the end of E2. Later, both values rose, reaching 131 mM Na^+ and 6.4 mM K^+ owing to

Table 1
Performances of the developed platform compared with previously reported ISFET-based wearables for sweat sensing.

REF	ISFETs	Fabrication	Sensitivity [mV decade^{-1}]	LOD	Microfluidics	Demonstrated length of continuous recording	On-body measurements validated with standard techniques	Readout system
(Jeon and Cho, 2020)	1 for pH	EG-ISFET of SnO_2 on an indium-gallium-zinc-oxide (InGaZnO) thin-film transistor, integrated into a flexible transparent PEN substrate	2364	pH 10[a]	No	NA[b]	No	No
(Park et al., 2021)	1 for Na^+	CNT-based ISFET with SiO_2 gate. Ag/AgCl ink and PVB membrane to obtain the RE on-chip	58.0[c]	10^{-4} M Na^+[a]	No	NA[b]	No	No
(Douthwaite et al., 2017)	9 for pH	Si_3N_4 ISFET array on a CMOS ASIC	13	pH 7[a]	No	NA[b]	No	Yes (thermoelectrically powered)
Garcia-Cordero et al. (2018)	32 for pH, Na^+ and K^+	ISFETs on ultrathin body fully depleted silicon-on-insulator substrate. Ag layer chlorinated and PVC membrane to obtain the solid-state RE	36 (pH-ISFET) 62 (Na-ISFET) 55 (K-ISFET)	pH 9[a] $5{\cdot}10^{-3}$ M Na^+[a] $5{\cdot}10^{-3}$ M K^+[a]	SU-8 microfluidics	NA[b]	No	No
Zhang et al. (2019)	1 for pH 1 for Na^+ 1 for K^+ 1 for Ca^{2+}	3D-EG-ISFETs integrated on a CMOS ASIC. Ag electrode chlorinated and PVB membrane to obtain the solid-state RE	57.2 (H-ISFET) −56.9 (Na-ISFET) −48.1 (K-ISFET) −25.7 (Ca-ISFET)	pH 8[a] 10^{-3} M Na^+[a] 10^{-3} M K^+[a] 10^{-4} M Ca^{2+}[a]	Fluidics + cotton absorbent	NA[b]	No (Sweat samples in vitro evaluation with Horiba devices)	Yes
Cazalé et al. (2016)	1 pH 1 for Na^+	SiO_2/Si_3N_4 ISFETs on a PI platform. Ag/AgCl-printed pseudo-RE	53.0 (pH-ISFET) 110.0 (Na-ISFET) (sensitivity 55 Na +55 Cl pseudo-RE)	pH 13[a] 10^{-5} M Na^+[a]	Textile-based sweat pump	1.5 h	Yes. But difference between methods not quantified	Yes
Nakata et al. (2017)	1 for pH	Al_2O_3 ISFET on InGaZnO thin-film, integrated on a PI platform. Ag/AgCl-printed pseudo-RE	51.2	pH 11.4[a]	No	250 s	Yes. But difference between methods not quantified	No
This work	1 for pH 1 for Na^+ 1 for K^+	Si_3N_4 ISFETs on a PI platform. Ag/AgCl ink and PVB membrane to obtain the solid-state RE	51.7 (pH-ISFET)[c] 57.1 (Na-ISFET)[c] 52.0 (K-ISFET)[c]	pH 12 10^{-5} M Na^+ 10^{-6} M K^+	PE/PP fibre fluidics	85 min	Yes. Quantified difference between methods	Yes

[a] Extracted from linear range.
[b] Not applicable.
[c] In artificial sweat.

the intensified cycling power and, consequently, the higher sweat rate. The pH sensor showed this increase when being in the middle of E3, shifting to 8.4.

At the end of E3, a fan was brought close to the subject to explore the impact of ambient temperature and evaporation on the sensor responses. This led to a sudden drop in temperature (down to 21.5 °C), coinciding with a slight decrease in the concentrations of the target analytes. Next, the fan was replaced with a heater and the skin temperature rose up to 30.7 °C. Although the ISFET sensor signals were noisier in this scenario, distinct increases in Na^+ and K^+ concentrations were evident, with sudden spikes of 180 mM and 11 mM, respectively. It is important to note that warmer conditions usually correspond to increased sweat rates and ion concentrations. However, existing studies suggest that skin temperature may also affect sweat composition, providing a potential explanation for the observed phenomena (Baker and Wolfe, 2020).

Finally, as the subject recovered from the exercise by cycling at a lower power, a decrease in skin temperature (25.6 °C) was noted. Correspondingly, both pH and Na^+ concentration steadily decreased to pH 7.5 and 105 mM, respectively. By contrast, the K^+ concentration remained constant at around 4.2 mM, regardless of the sweat flow rate.

The performance of the patch was compared with previously reported wearable platforms based on ISFETs for ion determination in sweat (Table 1). Among them only three presented results for multiple parameters and only two papers provide results for on-body measurements. Among them, only the work from Cazale et al. presents data for more than 1 h but results are not compared with a reference method. Besides, any of them measured pH, Na^+ and K^+ concentrations, jointly with skin temperature under continuous monitoring mode, together with a fluidic structure to ensure sample renewal.

4. Conclusions

ISFET sensor devices can be readily applied for measuring ion concentrations in sweat. pH, Na^+, and K^+ ISFETs were characterized in standard and artificial sweat solutions, demonstrating an overall good performance in the range of analyte concentrations present in sweat.

The pH, Na^+ and K^+ ISFET sensors, together with a temperature probe, and a solid-state reference electrode combined with a capillary-based microfluidic component were integrated into a wearable platform and tested on-body. The results demonstrate that the sensors were stable for at least 85 min, working under continuous flow conditions. The measurements show that pH and K^+ concentration remained nearly constant during the whole physical exercise, while Na^+ concentration increased during the continuous physical effort, as previously reported in the literature. Values obtained from the ISFETs correlated well with the values from the discrete sample collection during the exercise, analyzed with the commercial ISE devices. These results demonstrate that potentiometric sensors based on ISFET devices, combined with simple microfluidic approaches, could be a feasible method to attain the continuous measurement of chemical target species in sweat to monitor the health status of individuals during intense physical exercise.

CRediT authorship contribution statement

Meritxell Rovira: Writing – review & editing, Writing – original draft, Validation, Methodology, Investigation. **Céline Lafaye:** Validation, Methodology, Investigation. **Silvia Demuru:** Methodology, Investigation. **Brince Paul Kunnel:** Methodology, Investigation. **Joan Aymerich:** Methodology, Investigation. **Javier Cuenca:** Methodology, Investigation, Conceptualization. **Francesc Serra-Graells:** Supervision, Conceptualization. **Josep Maria Margarit-Taulé:** Investigation, Conceptualization. **Rubaiyet Haque:** Methodology, Investigation. **Mathieu Saubade:** Validation, Methodology, Investigation. **César Fernández-Sánchez:** Writing – review & editing, Writing – original draft, Supervision, Conceptualization. **Cecilia Jimenez-Jorquera:** Writing – review & editing, Writing – original draft, Supervision, Conceptualization.

Declaration of competing interest

The authors declare that they have no known competing financial interests or personal relationships that could have appeared to influence the work reported in this paper.

Data availability

Data will be made available on request.

Acknowledgements

This work was performed within the WeCare project, funded by the Swiss National Science Foundation (SNSF, Sinergia Program, Project CRSIIS_177255/1) and used the ICTS Network MICRONANOFABS supported by the Spanish Ministry of Science and Innovation. We would also like to thank Miwon, South Corea and Allnex for providing photocurable polymers. The authors acknowledge the participation in the Electrobionet network (ref. RED2022-134120-T) funded by MICIN/AEI/10.13039/501100011033).

Appendix A. Supplementary data

Supplementary data to this article can be found online at https://doi.org/10.1016/j.bios.2024.116560.

References

Anastasova, S., Crewther, B., Bembnowicz, P., Curto, V., Ip, H.M., Rosa, B., Yang, G.Z., 2017. A wearable multisensing patch for continuous sweat monitoring. Biosens. Bioelectron. 93, 139–145. https://doi.org/10.1016/j.bios.2016.09.038.

Baker, L.B., 2017. Sweating rate and sweat sodium concentration in athletes: a review of methodology and Intra/Interindividual variability. Sports Med. 47, 111–128. https://doi.org/10.1007/s40279-017-0691-5.

Baker, L.B., De Chavez, P.J.D., Nuccio, R.P., Brown, S.D., King, M.A., Sopeña, B.C., Barnes, K.A., 2022. Explaining variation in sweat sodium concentration: effect of individual characteristics and exercise, environmental, and dietary factors. J. Appl. Physiol. 133, 1250–1259. https://doi.org/10.1152/japplphysiol.00391.2022.

Baker, L.B., Ungaro, C.T., Barnes, K.A., Nuccio, R.P., Reimel, A.J., Stofan, J.R., 2014. Validity and reliability of a field technique for sweat Na+ and K+ analysis during exercise in a hot-humid environment. Phys. Rep. 2 https://doi.org/10.14814/phy2.12007.

Baker, L.B., Wolfe, A.S., 2020. Physiological mechanisms determining eccrine sweat composition. Eur. J. Appl. Physiol. 2020, 719–752. https://doi.org/10.1007/S00421-020-04323-7, 1204 120.

Bariya, M., Nyein, H.Y.Y., Javey, A., 2018. Wearable sweat sensors. Nat. Electron. 1, 160–171. https://doi.org/10.1038/s41928-018-0043-y.

Buono, M.J., Lee, N.V.L., Miller, P.W., 2010. The relationship between exercise intensity and the sweat lactate excretion rate. J. Physiol. Sci. 60, 103–107. https://doi.org/10.1007/s12576-009-0073-3.

Cao, S., Sun, P., Xiao, G., Tang, Q., Sun, X., Zhao, H., Zhao, S., Lu, H., Yue, Z., 2023. ISFET-based sensors for (bio)chemical applications: a review. Electrochem. Sci. Adv. 3, 1–25. https://doi.org/10.1002/elsa.202100207.

Cazalé, A., Sant, W., Ginot, F., Launay, J.C., Savourey, G., Revol-Cavalier, F., Lagarde, J. M., Heinry, D., Launay, J., Temple-Boyer, P., 2016. Physiological stress monitoring using sodium ion potentiometric microsensors for sweat analysis. Sensors Actuators B Chem 225, 1–9. https://doi.org/10.1016/J.SNB.2015.10.114.

Esashi, M., Matsuo, T., 1978. Integrated Micro multi ion sensor using field effect of semiconductor. IEEE Trans. Biomed. Eng. BME-25, 184–192. https://doi.org/10.1109/TBME.1978.326245.

Garcia-Cordero, E., Bellando, F., Zhang, J., Wildhaber, F., Longo, J., Guérin, H., Ionescu, A.M., 2018. Three-dimensional integrated Ultra-low-volume Passive microfluidics with ion-Sensitive field-effect transistors for Multiparameter wearable sweat Analyzers. ACS Nano 12, 12646–12656. https://doi.org/10.1021/acsnano.8b07413.

Ghaffari, R., Rogers, J.A., Ray, T.R., 2021. Recent progress, challenges, and opportunities for wearable biochemical sensors for sweat analysis. Sensors Actuators B Chem. B Chem. 332, 129447 https://doi.org/10.1016/j.snb.2021.129447.

Golparvar, A., Tonello, S., Meimandi, A., Carrara, S., 2023. Inkjet-printed Soft Intelligent medical Bracelet for Simultaneous real-time sweat potassium (K+), sodium (Na+), and skin temperature analysis. IEEE Sensors Lett 7. https://doi.org/10.1109/LSENS.2023.3267180.

Gutiérrez-Capitán, M., Baldi, A., Gómez, R., García, V., Jiménez-Jorquera, C., Fernández-Sánchez, C., 2015. Electrochemical nanocomposite-derived sensor for the analysis of

chemical oxygen demand in urban wastewaters. Anal. Chem. 87, 2152–2160. https://doi.org/10.1021/ac503329a.
Gutierrez, M., Llobera, A., Vila-Planas, J., Capdevila, F., Demming, S., Büttgenbach, S., Mínguez, S., Jimenez-Jorquera, C., 2010. Hybrid electronic tongue based on optical and electrochemical microsensors for quality control of wine. Analyst 135, 1718–1725. https://doi.org/10.1039/c0an00004c.
Jimenez-Jorquera, C., Orozco, J., Baldi, A., 2010. ISFET based microsensors for environmental monitoring. Sensors 10, 61–83. https://doi.org/10.3390/s100100061.
Margarit-Taulé, J.M., Martín-Ezquerra, M., Escudé-Pujol, R., Jiménez-Jorquera, C., Liu, S.-C., 2022. Cross-compensation of FET sensor drift and matrix effects in the industrial continuous monitoring of ion concentrations. Sensors Actuators B Chem. 353, 131123 https://doi.org/10.1016/J.SNB.2021.131123.
Matzeu, G., O'Quigley, C., McNamara, E., Zuliani, C., Fay, C., Glennon, T., Diamond, D., 2015. An integrated sensing and wireless communications platform for sensing sodium in sweat. Anal. Methods 8, 64–71. https://doi.org/10.1039/C5AY02254A.
Min, J., Tu, J., Xu, C., Lukas, H., Shin, S., Yang, Y., Solomon, S.A., Mukasa, D., Gao, W., 2023. Skin-interfaced wearable sweat sensors for precision medicine. Chem. Rev. 123, 5049–5138. https://doi.org/10.1021/acs.chemrev.2c00823.
Muñoz, J., Bratov, A., Mas, R., Abramova, N., Domínguez, C., Bartrolí, J., 1996. Planar compatible polymer technology for packaging of chemical microsensors. J. Electrochem. Soc. 143, 2020–2025. https://doi.org/10.1149/1.1836942.
Nakata, S., Arie, T., Akita, S., Takei, K., 2017. Wearable, flexible, and Multifunctional Healthcare device with an ISFET chemical sensor for Simultaneous sweat pH and skin temperature monitoring. ACS Sens. 2, 443–448. https://doi.org/10.1021/acssensors.7b00047.
Neal, R.A., Massey, H.C., Tipton, M.J., Young, J.S., Corbett, J., 2016. Effect of permissive dehydration on induction and decay of heat acclimation, and temperate exercise performance. Front. Physiol. 7, 564. https://doi.org/10.3389/fphys.2016.00564.
Parrilla, M., Ferré, J., Guinovart, T., Andrade, F.J., 2016. Wearable potentiometric sensors based on commercial Carbon fibres for monitoring sodium in sweat. Electroanalysis 28, 1267–1275. https://doi.org/10.1002/elan.201600070.
Patterson, M.J., Galloway, S.D.R., Nimmo, M.A., 2000. Variations in regional sweat composition in normal human males. Exp. Physiol. 85, 869–875. https://doi.org/10.1111/J.1469-445X.2000.02058.X.
Pirovano, P., Dorrian, M., Shinde, A., Donohoe, A., Brady, A.J., Moyna, N.M., Wallace, G., Diamond, D., McCaul, M., 2020. A wearable sensor for the detection of sodium and potassium in human sweat during exercise. Talanta 219, 121145. https://doi.org/10.1016/j.talanta.2020.121145.
Rollo, I., Randell, R.K., Baker, L., Leyes, J.Y., Leal, D.M., Lizarraga, A., Mesalles, J., Jeukendrup, A.E., James, L.J., Carter, J.M., 2021. Fluid balance, sweat Na+ Losses, and Carbohydrate Intake of elite Male Soccer Players in response to low and high training intensities in Cool and hot environments. Nutrients 13, 401. https://doi.org/10.3390/NU13020401.
Rovira, M., Lafaye, C., Wang, S., Fernandez-Sanchez, C., Saubade, M., Liu, S.C., Jimenez-Jorquera, C., 2023. Analytical assessment of sodium ISFET based sensors for sweat analysis. Sensors Actuators B Chem 393, 134135. https://doi.org/10.1016/J.SNB.2023.134135.
Sato, K., 1977. The physiology, pharmacology, and biochemistry of the eccrine sweat gland. Rev. Physiol. Biochem. Pharmacol. 79, 51–131. https://doi.org/10.1007/BFB0037089.
Schazmann, B., Morris, D., Slater, C., Beirne, S., Fay, C., Reuveny, R., Moyna, N., Diamond, D., 2010. A wearable electrochemical sensor for the real-time measurement of sweat sodium concentration. Anal. Methods 2, 342–348. https://doi.org/10.1039/b9ay00184k.
Schwartz, I.L., Thaysen, J.H., 1956. Excretion of sodium and potassium in human sweat. J. Clin. Invest. 35, 114–120. https://doi.org/10.1172/JCI103245.
Sonner, Z., Wilder, E., Heikenfeld, J., Kasting, G., Beyette, F., Swaile, D., Sherman, F., Joyce, J., Hagen, J., Kelley-Loughnane, N., Naik, R., 2015. The microfluidics of the eccrine sweat gland, including biomarker partitioning, transport, and biosensing implications. Biomicrofluidics 9, 1–19. https://doi.org/10.1063/1.4921039.
Wang, S., Lafaye, C., Saubade, M., Besson, C., M Margarit-Taule, J., Gremeaux, V., Liu, S. C., 2022. Predicting hydration status using machine learning models from physiological and sweat biomarkers during endurance exercise: a single case study. IEEE J. Biomed. Heal. Informatics 26, 4725. https://doi.org/10.1109/JBHI.2022.3186150.
Wang, S., Rovira, M., Demuru, S., Lafaye, C., Kim, J., Kunnel, B.P., Besson, C., Fernandez-Sanchez, C., Serra-Graells, F., Margarit-Taule, J.M., Aymerich, J., Cuenca, J., Kiselev, I., Gremeaux, V., Saubade, M., Jimenez-Jorquera, C., Briand, D., Liu, S.C., 2023. Multisensing wearables for real-time monitoring of sweat electrolyte biomarkers during exercise and analysis on their correlation with core body temperature. IEEE Trans. Biomed. Circuits Syst. https://doi.org/10.1109/TBCAS.2023.3286528.
Weschler, L.B., 2008. Sweat electrolyte concentrations obtained from within occlusive coverings are falsely high because sweat itself leaches skin electrolytes. J. Appl. Physiol. 105, 1376–1377. https://doi.org/10.1152/JAPPLPHYSIOL.00924.2007.
Xu, G., Cheng, C., Liu, Z., Yuan, W., Wu, X., Lu, Y., Low, S.S., Liu, J., Zhu, L., Ji, D., Li, S., Chen, Z., Wang, L., Yang, Q., Cui, Z., Liu, Q., 2019. Battery-free and wireless Epidermal electrochemical system with all-printed stretchable electrode array for multiplexed in situ sweat analysis. Adv. Mater. Technol. 4, 1–13. https://doi.org/10.1002/admt.201800658.
Yang, D.S., Ghaffari, R., Rogers, J.A., 2023. Sweat as a diagnostic biofluid. Science 379, 760–761. https://doi.org/10.1126/SCIENCE.ABQ5916 (80-).
Yang, M., Sun, N., Lai, X., Wu, J., Wu, L., Zhao, X., Feng, L., 2023. Paper-based Sandwich-Structured wearable sensor with Sebum filtering for continuous detection of sweat pH. ACS Sens. 8, 176–186. https://doi.org/10.1021/acssensors.2c02016.
Yokus, M.A., Songkakul, T., Pozdin, V.A., Bozkurt, A., Daniele, M.A., 2020. Wearable multiplexed biosensor system toward continuous monitoring of metabolites. Biosens. Bioelectron. 153, 112038 https://doi.org/10.1016/J.BIOS.2020.112038.
Zhang, J., Rupakula, M., Bellando, F., Garcia Cordero, E., Longo, J., Wildhaber, F., Herment, G., Guérin, H., Ionescu, A.M., 2019. Sweat biomarker sensor incorporating Picowatt, three-Dimensional extended metal gate ion sensitive field effect transistors. ACS Sens. 4, 2039–2047. https://doi.org/10.1021/acssensors.9b00597.
Zhao, J., Lin, Y., Wu, J., Nyein, H.Y.Y., Bariya, M., Tai, L.C., Chao, M., Ji, W., Zhang, G., Fan, Z., Javey, A., 2019. A fully integrated and Self-Powered Smartwatch for continuous sweat glucose monitoring. ACS Sens. 4, 1925–1933. https://doi.org/10.1021/acssensors.9b00891.